Selective Monohydrolysis of Bridged and Unbridged Calix[4]arene Esters and its Inhibition by Alkali Ion. Evidence for Hydronium Ion Complexation

Geraldine Barrett,[b] Volker Bohmer,*[,a] George Ferguson,[c] John F. Gallagher,[d] Stephen J. Harris,[d] Raymond G. Leonard,[d] M. Anthony McKervey,*[,b] Michael Owens,[b] Moniralsadat Tabatabai,[a] Anita Vierengel[a] and Walter Vogt[a]

[a] *Institute for Organic Chemistry, Johannes-Gutenberg University, J.-J. Becher Weg 34 SB1, 65 Mainz, Germany*

[b] *School of Chemistry, The Queen's University, Belfast BT9 5AG, N. Ireland, UK*

[c] *Department of Chemistry and Biochemistry, University of Guelph, Guelph, Ontario NIG 2W1, Canada*

[d] *Loctite (Ireland) Ltd., Research and Development, Whitestown Industrial Estate, Tallaght, Dublin 24, Ireland*

Several bridged and unbridged calix[4]arene tetraester derivatives are hydrolysed by trifluoroacetic acid in chloroform with the loss of one, and only one, ester group to form triester monoacids. In bridged tetraethyl ester **11**, the group that is hydrolysed is that on the aromatic moiety not carrying the methylene bridge. The hydrolysis process is inhibited by the presence of alkali metal cations, especially sodium. Evidence is presented in favour of a hydrolytic process involving hydronium ion complexation within the hydrophilic oxygenated cavity of the calixarene receptor. Crystals of the triester monoacid **5** were studied at 123 K and are monoclinic, space group $P2_1/n$, with four molecules in a cell of dimensions $a = 13.554(6)$, $b = 20.095(9)$, $c = 20.658(17)$ Å, $\beta = 102.27(5)°$. The structure was solved by direct methods and refined by full-matrix least-squares calculations; $R = 0.063$ for 2017 observed reflections. The calix[4]arene has a distorted cone conformation similar to that found in other closely related derivatives. The hydroxy group of the carboxylic acid moiety is hydrogen bonded [O - - - O 2.722(10) Å] to a proximal ethereal oxygen and not to carbonyl oxygen atoms.

There is now substantial evidence to support the view that some chemically modified calix[4]arenes of the type shown in **1** utilise their ethereal and carbonyl oxygen atoms as receptor sites in forming complexes with alkali and alkaline earth cations.[1,2] The carbonyl oxygen atoms may be present in the form of esters,[3] ketones,[4] carboxylic acids[5] or amides,[6] the cone conformation **2** of the tetramer ensuring that the ligating arms of the receptor are suitably preorganised for cation reception. X-Ray diffraction studies of several examples of **1** and of the KSCN complex of tetra-amide **3** support this interpretation.[6] The selectivity of complexation is a function of the nature of the carbonyl-containing functionality.[2] Phase-transfer studies and stability constant measurements (in methanol) with tetraethyl ester **4** reveal a high selectivity for Na^+ over the other alkali cations.[3] Although a stronger binder, amide **3** is less selective than ester **4** for Na^+ with respect to K^+, with a stability constant (β) ratio of 130 as compared with

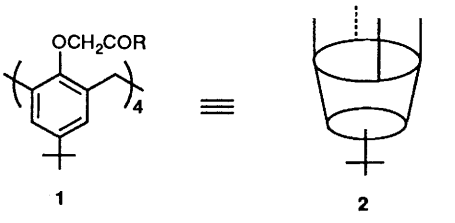

1 ≡ **2** (Cone conformation)

3; R = NEt_2
4; R = OEt
6; R = OBu^t
8; R = OMe
9; R = OCH_2COPh

400 for ester **4**.[2] Another feature of the complexation preference exhibited by the tetraester is that its Na^+ complex is much more stable kinetically than is its K^+ counterpart. The latter fact is pertinent to the work reported here.[7]

In the course of a study of the influence of acids on the stability of tetraester **4** we observed an unexpectedly rapid reaction with trifluoroacetic acid (TFA) in chloroform at room temperature which could be followed conveniently by ^1H NMR spectroscopy. Spectral changes for the aromatic region were observed when **4** in $CDCl_3$ was treated with TFA. Immediately after mixing the spectrum revealed the formation of a new substance (20% conversion after 2–3 min) in which the four-fold symmetry of **4** had been replaced by a symmetry plane resulting in two singlets and one AB system in the aromatic region. Furthermore, some of the signals attributable to unreacted ester showed small but significant changes in their chemical shifts (see Table 1). After *ca.* 1 h the conversion was >90% completed and over an additional 24 h period no further changes could be detected by NMR spectroscopy. A preparative scale experiment yielded a crystalline substance, m.p. 166–168 °C (88% yield) which was homogeneous by HPLC analysis. It quickly became clear from the NMR data that the product was triester monoacid **5**.

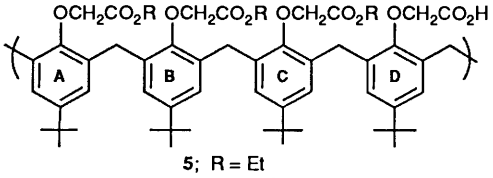

5; R = Et
7; R = Bu^t

Two of the more intriguing aspects of the reaction were its apparent ease (a simple model ethyl ester, ethyl *p-tert*-butylphenoxyacetate, showed no measurable instability in TFA under comparable conditions) and its abrupt termination after

Table 1 Chemical shifts (in ppm) of the unreacted tetraester **4** and conversion (in % after 4 min) to the monoacid **5** for different concentrations of TFA [a]

			$Ar-CH_2-Ar$		CH_2-CH_3			
$c(TFA)/c(4)$	Ar–H	CH_2–CO	H_A	H_B			$C(CH_3)_3$	%
0	6.75	4.78	4.84	3.17	4.19	1.27	1.05	
(*a*)								
0.33	6.76	4.79	4.74	3.18	4.21	1.27	1.05	18
1.3	6.77	4.80	4.67	3.19	4.23	1.28	1.06	30
3.9	6.78	4.82	4.62	3.20	4.24	1.28	1.06	23
11.7	6.79	4.83	4.60	3.21	4.26	1.28	1.06	17
(*b*)								
0.33	6.76	4.78	4.76	3.18	4.20	1.27	1.05	22
0.66	6.76	4.79	4.73	3.18	4.20	1.27	1.05	31
1.3	6.77	4.80	4.68	3.19	4.22	1.27	1.05	50
3.9	6.78	4.81	4.63	3.20	4.24	1.28	1.06	44
18.2	6.82	4.83	4.58	3.23	4.28	1.29	1.07	19
	(+0.06	+0.05	−0.25	+0.06	+0.09	+0.03	+0.02)	
(*c*)								
LiSCN	7.04	4.81	4.61	3.36	4.43	1.38	1.12	
	(+0.29	+0.03	−0.22	+0.19	+0.24	+0.12	+0.07	
NaSCN	7.09	4.45	4.22	3.37	4.35	1.39	1.11	
	(+0.34	−0.34	−0.62	+0.20	+0.16	+0.12	+0.06)	

[a] The commercial $CDCl_3$ used for the measurements in Table 1(*a*), was saturated with water for the measurements in Table 1(*b*). For the highest TFA concentration the values in parentheses are the differences from the free ligand in the absence of TFA (first line). In Table 1(*c*) are presented chemical shifts (in ppm) for the Li and Na complex of tetraester **4** ($CDCl_3$ solution of **4**, saturated by shaking with solid LiSCN and NaSCN). In parentheses the differences relative to pure **4** are indicated, which should be compared to the differences observed for the highest concentration of TFA [last line of Table 1(*b*)].

removal of one, and only one, of the four ester functions. An indication of which features of **4** might be responsible was provided when a $CDCl_3$ solution of the tetraester was saturated with sodium thiocyanate (or sodium iodide) prior to the addition of TFA, for with this modification no detectable amounts of hydrolysis could be observed over a ten-day period. Clearly, the sodium complex of **4**, which we knew independently was capable of existence,[3] and whose presence in the $CDCl_3$ solution could be confirmed by NMR spectroscopy prior to the addition of TFA, does not react with the acid. A similar effect was observed using lithium thiocyanate. A pertinent third aspect of the reaction was that ethanol was produced, though with time it was transformed into its trifluoroacetate, thus establishing that the process was one of hydrolysis by adventitious water and not *trans*-esterification.

The behaviour of the tetraester in the presence of potassium thiocyanate presented a contrasting picture. When a solution of **4** was shaken with KSCN a ^1H NMR spectrum was obtained with very broad signals which were tentatively assigned as follows: δ_H; 1.073 (s, Bu^t), 1.312 (t, CH_3 of Et), 3.245 (d, J = 12.5 Hz, $ArCH_2Ar$), 4.273–4.260 (broad with an indication of splitting, CH_2 of Et), 4.648 (s, OCH_2CO and $ArCH_2Ar$) and 6.895 (s, ArH). Clearly these values are intermediate between those of the free tetraester and its Na^+ complex (see Table 1), with the broadening most pronounced for the signals for those hydrogen atoms which are most affected during complex formation with KSCN. When TFA was added to the $CDCl_3$ solution hydrolysis ensued immediately though it was observed to level off in rate at *ca.* 55% conversion. The following data were obtained with a concentration of **4** of 0.017 mol dm^{-3} and of TFA of 0.022 mol dm^{-3} (concentrations ±10%), time with % conversion in parentheses: 3 min (14%), 7 min (28%), 40 min (53%), 4 h (62%), 27 h (71%), 49 h (77%) and 120 h (83%). Over the hydrolysis period a very pronounced sharpening of the ^1H NMR signals occurred. We interpret this behaviour as indicating that in the first place, prior to the addition of TFA, there is an incomplete uptake of KSCN by the tetraester in forming the complex and that there is an exchange between the free ligand and the complex at a rate appropriate to the observed NMR line shape. Addition of TFA initiates hydrolysis, but it is the free tetraester that is being consumed. The K^+ ion in solution is restricted to the remaining tetraester which now shows the sharp signals of a K^+ complex which cannot exchange, all the free ligand having been consumed by TFA. The similarity of the NMR spectrum of the K^+ complex to that of the Na^+ complex is striking with only minute differences in the respective δ_H values. This interpretation was confirmed by a simple experiment: after the 'line sharpening' effect had been observed on addition of TFA, a fresh solution of tetraester was added to the $CDCl_3$ solution, whereupon an immediate broadening of the ^1H signals again occurred.

A series of measurements in which the ^1H NMR spectrum of **4** and the % conversion to **5** after 4 min were recorded as a function of TFA concentration also proved to be informative (Table 1). The measurements were first made using spectroscopic grade $CDCl_3$ as the solvent and then repeated with $CDCl_3$ saturated with water. The two sets of results are presented in Tables 1(*a*) and 1(*b*). TFA induces minor spectral changes in **4**, the most distinctive being the shift to higher field of the doublet of the axial methylene protons (a part of the AB system). The important fact is that all these chemical shifts for **4** change continuously with increasing TFA concentration, while the percentage conversion to monoacid **5** goes through a maximum value. This maximum value in the reaction rate, which is higher for the water-saturated chloroform, occurs when the concentration ratio of TFA to tetraester is approximately unity. For comparison, Table 1 also contains the ^1H NMR spectra of the Li^+ and Na^+ complexes of **4** (solutions saturated with LiSCN and NaSCN, respectively). It is evident that all the signals of **4** are shifted by TFA in the direction of those of the Li^+ complex. These shifts, which are larger for Li^+ in most instances, are all to lower field with the exception of that for the axial methylene protons. The Na^+ complex, showing an even larger upfield shift for these axial protons,

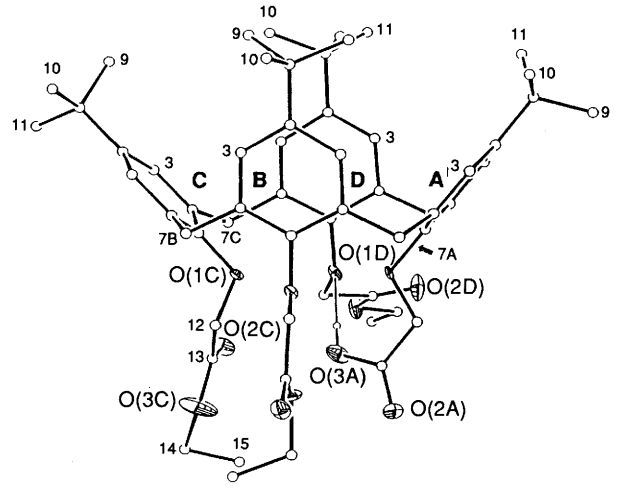

Fig. 1 A general view of **5** showing the crystallographic numbering scheme. For clarity, hydrogen atoms are omitted except for the carboxyl H atom; carbon atoms and the H atom are shown as small spheres of arbitrary size. The oxygen atoms are shown with 35% probability ellipsoids.

differs mainly with respect to the OCH_2CO signal which is shifted significantly upfield, whereas small downfield shifts are observed for the Li^+ complex and the TFA–tetraester solution.

These facts can be accommodated by a hydrolysis process which is initiated by the reversible complexation of a hydronium ion inside the hydrophilic cavity of **4** in much the same way that the Li^+ or Na^+ ion is encapsulated. The fact that all shifts induced by TFA are more pronounced at higher TFA concentrations indicates that a rapid equilibrium is operating. Attack by water from the outside of the cavity leads to hydrolysis. The rate of hydrolysis, however, falls off with higher TFA concentrations [Table 1(*a*) and 1(*b*)] which is also consistent with attack by water on the complexed hydronium ion, since the concentration of 'free water' will decrease with increasing concentration of hydronium ion. Sodium ion inhibits hydrolysis by complete complex formation with the tetraester: when the calixarene cavity is thus occupied, hydronium ion complexation is precluded and hydrolysis cannot occur. The same is apparently the case with lithium ion, although complete complexation cannot be deduced *a priori* from the ^1H NMR spectrum since this complex is not kinetically stable on the NMR time scale. Potassium ion, on the other hand, incompletely forms a complex with **4** which is rapidly exchanging with the free ligand. In the presence of TFA there is now competition with hydronium ion complexation and hydrolysis ensues. Hydrolysis was not observed in dioxane or aqueous dioxane, solvents where solvation of the hydronium ion would be expected to compete with its complexation by the tetraester. The behaviour in benzene, on the other hand, was very similar to that in chloroform.

Selective monohydrolysis was also observed with several other calix[4]arene tetraesters including the *tert*-butyl derivative **6**. Normally *tert*-butyl esters are cleaved rapidly by TFA, unlike their *n*-alkyl counterparts (*cf.* ethyl phenoxyacetate above), in a process which is believed to be one of alkyl–oxygen fission. Thus, while *tert*-butyl ester **6** was indeed much more reactive in TFA than the ethyl ester **4**, its behavioural pattern suggested that the alkyl–oxygen cleavage mechanism was not operating to a significant extent, otherwise one might have anticipated a random successive cleavage of all four ester functions. In fact, *tert*-butyl ester **6** underwent clean monohydrolysis to **7** which was *ca.* 90% completed after *ca.* 3 min (*cf.* the ethyl ester which showed 20% conversion after 3 min). The process was essentially complete in 10 min, though over longer periods further cleavage of the monoacid tri-*tert*-butyl ester **7** was observed as one might have expected if the normal mechanism of *tert*-butyl ester hydrolysis in TFA now becomes increasingly operative. The Na^+ complex of tetra-*tert*-butyl ester was prepared in $CDCl_3$ and found to be completely inert to TFA over a 30 h period. In another experiment in which a mixture of Na^+–*tert*-butyl ester complex and free ligand in $CDCl_3$ was treated with TFA it was observed that only cleavage of the free ligand occurred. Similar behaviour was observed with the tetramethyl and tetraphenacyl esters **8** and **9**. In these and other examples to be discussed later, experiments were conducted on an NMR scale only. The ^1H spectra of the TFA reaction products in $CDCl_3$ were each sufficiently well resolved to permit unequivocal assignments of the monoacid structure in each case, though the products were not isolated.

It is significant that in the examples discussed above hydrolysis effectively ceases after one ester cleavage. This may suggest that in the triester monoacid complexation of H_3O^+ within the cavity is now prohibited and consequently further attack by water does not occur. The reason for this may be associated with the structure and acidity of the monoacid. ^1H NMR data clearly indicate that monoacid **5** in solution possesses a cone conformation which is much distorted in comparison with that of the tetraethyl ester. In particular, the chemical shifts of the aromatic ring protons of the two distal ester ring residues (rings **B** and **D** in Fig. 1) as compared with those of the third ester ring (ring **C**) and the acid bearing ring (ring **A**) suggest that the former pair are almost parallel to each other, whereas the latter pair are inclined, though not to the same degree, towards the inside of the cavity. This arrangement should facilitate intramolecular hydrogen bond formation between the carboxylic acid group and the oxygen atom of an ether or ester function. Support for this interpretation is provided by the pK_a of monoacid **5** which in methanol was found to be 10.0, *ca.* 3 pK_a units more than phenoxyacetic acid in the same solvent.[8] The monoacid is thus the weaker acid which is explicable if the monoacid has additional stabilisation of the unionised form resulting from intramolecular hydrogen bonding. This interpretation of the solution conformation of **5** finds strong further support from X-ray diffraction analysis of the crystal.

The distorted cone conformation adopted in the solid state by the triester monoacid is shown in Fig. 1. The carboxyl hydroxy group (O3A–H) is clearly hydrogen bonded to the proximal phenolic oxygen O1D [O---O separation 2.722(10) Å, hydroxy H atom clearly visible in a difference map on the O3A---O1D line of centres]. The molecular conformation of **5** may be defined by the angles that the four aromatic rings **A**–**D** make with the macrocyclic ring methylene groups: **A** [129.1(3)°], **B** [95.0(3)°], **C** [131.3(3)°] and **D** [92.9(3)°] (interplanar angles >90° indicate that the ring system is tilted so that its *tert*-butyl group is directed away from the ring cavity). Rings **B** and **D** are thus almost parallel [interplanar angle 7.9(4)° and tilted so as to increase the *tert*-butyl---*tert*-butyl separation], while rings **A** and **C** are almost normal to one another [interplanar angle 80.4(4)°]. Similar conformations have been found in related calix[4]aryl esters.[9] This conformation leads to oxygens O1A and O1C being separated by 3.720(10) Å; the O1B---O1D separation is 5.242(10) Å. The O---O distances between adjacent phenolic O atoms are in the range 3.051(10) to 3.358(10) Å. There are only two intramolecular interchain O---O contacts <3.3 Å within the calix[4]arene cavity, O3A---O1C [3.250(10) Å] and O3A---O2C [3.178(10) Å]. The ester side group off ring **D** (whose ether oxygen O1D is involved in the intramolecular hydrogen bonding) is *exo*-oriented while the ester functions off rings **B** and **C** lie mostly below the calixarene cavity. In all cases the methylene carbon (C12) bonded to ether oxygen O1 is

Table 2 Summary of bond lengths/Å for **5**

Bond	Range	Mean
C_{ar}–O	1.400(11)–1.431(11)	1.411
C_{sp^3}–O	1.405(13)–1.433(11)	1.422
CH_2–C_{sp^2}	1.475(15)–1.531(16)	1.503
C_{sp^2}=O	1.191(13)–1.223(13)	1.205
C_{sp^2}–O	1.314(13)–1.342(14)	1.331
C_{sp^3}–O	1.459(13)–1.723(21)	1.563
Ethyl C–C	1.381(23)–1.488(16)	1.441
C_{ar}–CH_2	1.479(14)–1.527(13)	1.503
C_{ar}–C_{Bu^t}	1.535(13)–1.544(13)	1.539
Butyl C_{sp^3}–C_{Me}	1.405(18)–1.564(16)	1.509
Aromatic C–C	1.348(14)–1.436(14)	1.391

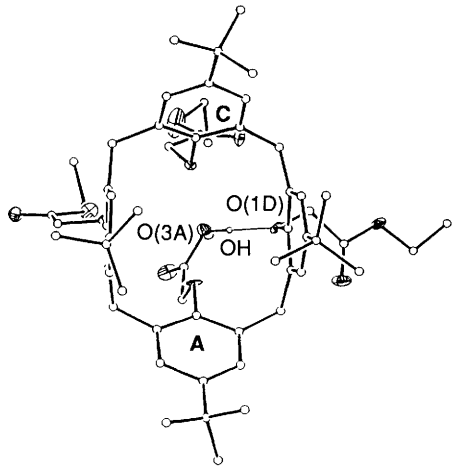

Fig. 2 A view of **5** viewed almost normal to the plane of the four CH_2 groups which link the four aromatic rings showing the intramolecular hydrogen bond

oriented *exo* to the appropriate aromatic ring plane [torsion angles C12–O1–C1–C2 being −82.5(8), −97.2(9), −114.1(9), −117.0(9)° for rings **A**–**D**, respectively]. Another feature of the structure is that in the three ester side chains the carbon and oxygen atoms of the O–CH_2–C(=O)–O–CH_2 moieties are essentially coplanar, with the carbonyl C=O group and the ethyl CH_2 group *cis*. In the ring **B** side chain, phenolic oxygen O1B is *trans* to carbonyl oxygen O2B, whereas in the **C** and **D** ring side chains, the phenolic and carbonyl oxygens are *cis*. Molecular dimensions (bond lengths are summarised in Table 2) are unexceptional (except for those associated with the markedly anisotropic/disordered atoms noted below in the Experimental section) and serve to establish the structure and the conformation of the hydrolysis product as the monoacid in a distorted cone.

The behaviour of the tetraester **10**[10] on exposure to TFA

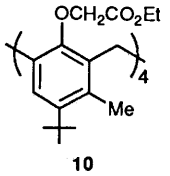

10

supports the above arguments based on conformation changes in the monoacid. Tetraester **10**, which is chiral by virtue of the presence of *meta* methyl substituents, exhibits a ^{1}H NMR spectrum with broad signals consistent with interconversion of two equivalent C_2 conformations at a rate comparable to that of the NMR time scale; in fact at −80 °C the aromatic protons, for example, appear as two singlets. This suggests that the usual C_{4v} symmetry exhibited by tetraesters without *meta* substituents, *e.g.* tetraethyl ester **4**, may result from a rapid interconversion of two equivalent C_{2v} conformations which have been found for all cone conformations in the crystalline state. Thus, at 400 MHz, the aromatic protons of **10** appear as a very broad absorption at δ 5.6–6.6, whereas the corresponding absorptions in tetraester **4** appear as a sharp singlet at δ 6.76. Upon addition of TFA to **10** monohydrolysis occurred at a rate significantly slower than that of **4**, yielding a product with an NMR pattern in the aromatic region of two singlets at δ 6.88 and 6.87 (corresponding to the former pair of singlets in the hydrolysis product of **4**) and two singlets at δ 5.87 and 5.76 (corresponding to the pair of doublets in **4**). This spectrum, in contrast to that of its precursor, consists of sharp signals and though complex, because all the CH_2 groups are non-equivalent and contain diastereotopic protons, it confirms the conformation of the hydrolysis product as a distorted cone with an intramolecular hydrogen bond similar to that shown in Fig. 2.

Conformational effects are also believed to be important in determining the behaviour of several *para*-bridged tetraesters **11**[11] on exposure to TFA, but here we have an additional selectivity with respect to the choice of ester group which is cleaved. In this series, in which methylene chains (n = 5, 7–9) span the *para* positions of two distal aromatic rings, two types of ester residue are present: two which are attached to the phenolic units carrying the *para* bridge and two which are attached to the phenolic groups not involved in bridging. Consequently, two structurally distinct monohydrolysis products are possible in each case. Compounds with R = *p-tert*-butyl were studied. In all cases monohydrolysis was observed cleanly with little or no further hydrolysis over a 24 h period. Furthermore, the same ^{1}H NMR pattern was observed in the products in the aromatic region as that observed with the unbridged triester monoacid **5**. In the *tert*-butyl region there appeared two singlets, closely separated ($\Delta\delta$ = 0.018–0.004 ppm) showing that the two phenolic units not involved in bridging are now non-equivalent; this non-equivalence is explicable if one of these two units is attached to the carboxylic acid function and the other an ester function. The remainder of the ^{1}H NMR spectra were consistent in detail with monoacid structure **12**, as shown for one example (n = 9) in Fig. 3. Analogous behaviour was observed with a series of three

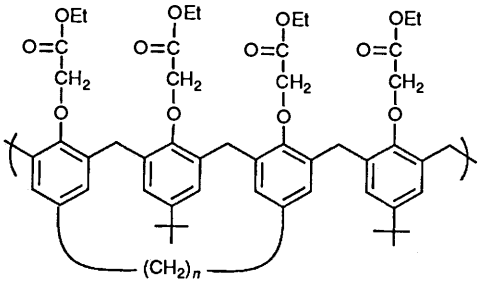

11

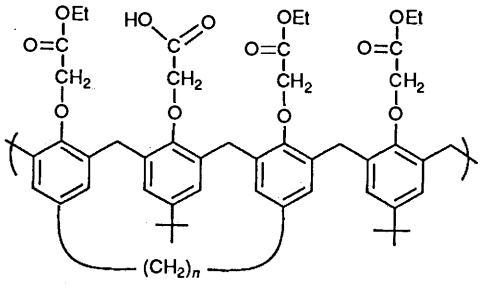

12

n = 5, 7–9

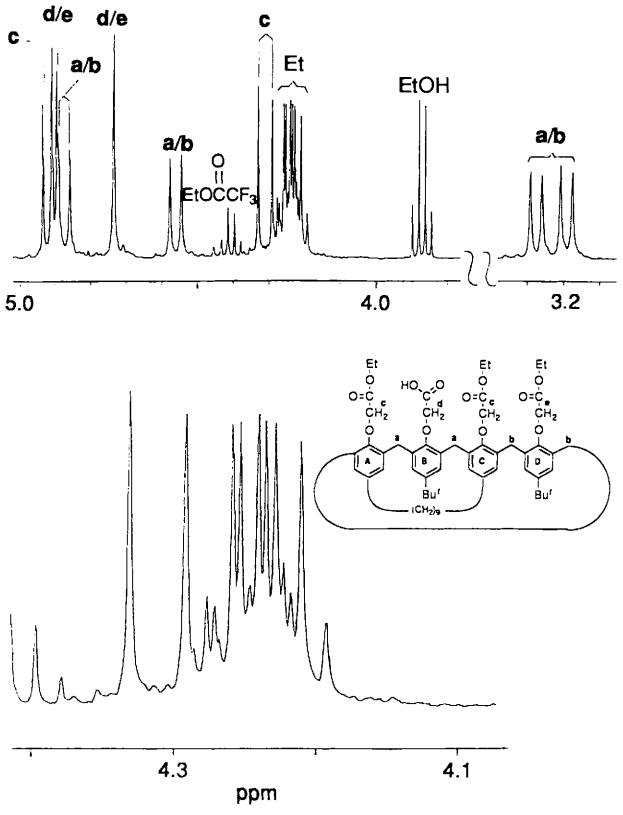

Fig. 3 ^{1}H NMR spectrum of hydrogen atoms **a**, **b**, **c** and **d** of monoacid **12**

bridged esters with *para* methyl groups,[12] the methyl singlet in the tetraester becoming two singlets in the product monoacid. Connection of the two opposite *para* positions bends the oxygen region of these phenolic units outwards while the unbridged phenolic units move towards the cavity. This is just the distortion found in the resulting monoacid, which may be the reason for the observed selectivity. In the bridged ester series it was also established that Na^+ complexation prior to exposure to TFA prevents hydrolysis. Approximate rate measurements for the TFA hydrolysis indicated that all bridged esters reacted at about the same rate and similar to that of the unbridged ester series, the difference being less than a factor of 3. This result is surprising when compared with the thermodynamic data for complexation of the bridged esters with Na^+ in methanol where stability constants range from <10 ($n = 5$) to $>10^6$ ($n = 8$). In the bridged ester series it was also established that Na^+ complexation prior to exposure to TFA prevented hydrolysis.

Selective monohydrolysis has also been observed with other calixarene derivatives. The mixed diester–diketone **13**[13] is cleaved once by TFA to produce monoacid–diketone **14**. Diester–diketone **13** is a good Na^+ receptor, a property shared with the related diester–diamide **15** which, however, is not cleaved by TFA. In the latter case we believe that the hydronium ion in the cavity is much more localised in the vicinity of the amide carbonyl, leaving the ester carbonyls much less activated for attack by water as compared with the situation in the tetraester. Apart from interest in the mechanism and mode of complexation, this selective hydrolysis of calixarene tetraesters to form monoacid triesters opens up synthetic routes to more elaborate systems, *e.g.* double calixarenes,[14] polymeric calixarenes,[15] and several calixarenes with mixed functionality.[2,16]

Experimental

M.p.s were determined on a Thomas Hoover apparatus and are uncorrected. ^{1}H NMR spectra were recorded at 400 MHz with tetramethylsilane as internal standard. *J* values are given in Hz. Elemental analyses were performed by the Microanalysis Laboratory, University College, Cork. The drying agent employed was magnesium sulfate. Tetraethyl ester **4** was prepared from *p-tert*-butylcalix[4]arene and ethyl bromoacetate according to the literature procedure.[3]

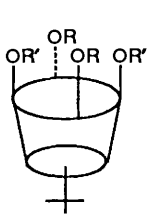

13; R = CH_2CO_2Et
R' = CH_2COCH_3

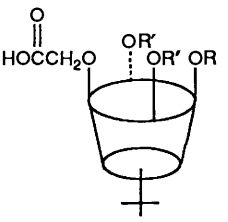

14; R = CH_2CO_2Et
R' = CH_2COCH_3

15; R = CH_2CO_2Et
R' = CH_2CONEt_2

Monohydrolysis of 5,11,17,23-*Tetra*-tert-*butyl*-25,26,27,28-*tetrakis*(*ethoxycarbonylmethoxy*)*calix*[4]*arene* (**4**)* *with TFA.*—A solution of **4** (5.01 g, 5.05 mmol) in chloroform (100 cm^3) was treated with trifluoroacetic acid (0.2 cm^3). The solution was stirred at room temperature for 24 h without exclusion of moisture and then was washed with water. The dried solution was concentrated to leave a white solid which on crystallisation from ethanol–water furnished 5,11,17,23-tetra-*tert*-butyl-28-carboxy-25,26,27-tris(ethoxycarbonylmethoxy)calix[4]arene (**5**) as white crystals, m.p. 166–169 °C (Found: C, 72.3; H, 7.7. $C_{58}H_{76}O_{12}$ requires C, 72.2; H, 7.8%); $\delta_H(CDCl_3)$ 7.143 (2 H, s, ArH), 7.133 (2 H, s, ArH), 6.621 (2 H, d, J_{AB} = 2.36, ArH), 6.526 (2 H, d, J_{AB} = 2.36), 4.939 (2 H, s, OCH_2CO), 4.859 (2 H, d, J_{AB} = 15.7, OCH_2CO), 4.574 (2 H, s, OCH_2CO), 4.350 (2 H, d, J_{AB} = 15.7, OCH_2CO), 4.963 (2 H, d, J = 12.8, $ArCH_2Ar$), 4.589 (2 H, d, J = 12.4, $ArCH_2Ar$), 3.248 (2 H, d, J_{AB} = 12, $ArCH_2Ar$), 3.187 (2 H, d, J_{AB} = 12.9, $ArCH_2Ar$), 4.251 (4 H, q, J_{AB} = 7.2, CH_2 of Et), 1.300 (6 H, t, J_{AB} = 6.5–7.2, CH_3 of Et), 1.285 (3 H, t, J_{AB} = 7.2–7.9, CH_3 of Et), 1.316 (9 H, s, Bu^t), 1.305 (9 H, s, Bu^t) and 0.815 (18 H, s, Bu^t).

25,26,27-*Tris*(tert-*butoxycarbonylmethoxy*)-5,11,17,23-*tetra*-tert-*butyl*-26-*carboxycalix*[4]*arene* (**7**).—A solution of 25,26,-27,28-tetrakis(*tert*-butoxycarbonylmethoxy)-5,11,17,23-tetra-*tert*-butylcalix[4]arene (**6**) (0.205 g, 1.85 10^{-4} mol) in chloroform (3 cm^3) was treated with trifluoroacetic acid (5 drops) and the solution was stirred in an open flask for 3 min. Water (5 cm^3) was then added and the mixture was shaken. The organic phase was washed twice with water (5 cm^3), dried and concentrated to a solid residue which on crystallisation from methanol–water furnished the monoacid tri-*tert*-butyl ester **7** (0.160 g, 82%), m.p. 184–185 °C (Found: C, 73.1; H, 8.0. $C_{64}H_{88}O_{12}$ requires C, 73.4; H, 8.5%); ν_{max}(KBr)/cm^{-1} 1760 and 1740; $\delta_H(CDCl_3)$ 0.847 (9 H, s, Bu^t), 1.336 and 1.342 (27 H, 2 s, Bu^t), 1.500 (18 H, s, Bu^t ester), 1.545 (9 H, s, Bu^t ester), 3.288–3.288 (2 H, dd, H_B, $ArCH_2$), 4.261, 4.312 (2 H, d, H_B, $ArCH_2$), 4.623 (2 H, s, OCH_2), 4.683, 4.726 (1 H, d, H_A, $ArCH_2$), 4.821 (6 H, s, OCH_2), 4.821, 4.871 (24, d, H_A, $ArCH_2$), 5.022, 5.065 (1 H, d, H_A, $ArCH_2$), 6.546, 6.553 (4 H, dd, ArH) and 7.156, 7.164 (4 H, d, ArH).

Good quality crystals of **5** were very difficult to obtain. Eventually, small crystals were obtained by slow evaporation

* For nomenclature, see *J. Chem. Soc., Perkin Trans. 2*, 1992, 1119.

Table 3 Positional parameters and their esds in parentheses

Atom	*x*	*y*	*z*
O(1A)	0.9291(5)	0.6360(3)	0.1022(3)
O(2A)	1.0380(5)	0.6290(4)	−0.0386(3)
O(3A)	0.9264(6)	0.6985(4)	−0.0115(3)
C(1A)	0.9485(7)	0.6119(5)	0.1689(4)
C(2A)	0.9237(7)	0.5467(5)	0.1802(4)
C(3A)	0.9444(8)	0.5251(5)	0.2463(5)
C(4A)	0.9866(7)	0.5683(5)	0.2985(5)
C(5A)	1.0068(8)	0.6322(6)	0.2836(5)
C(6A)	0.9896(7)	0.6570(5)	0.2188(5)
C(7A)	0.8670(7)	0.5044(5)	0.1265(5)
C(8A)	1.0044(8)	0.5425(5)	0.3702(4)
C(9A)	1.1152(13)	0.5361(11)	0.3961(7)
C(10A)	0.9549(16)	0.4829(9)	0.3792(6)
C(11A)	0.9718(15)	0.5925(8)	0.4148(6)
C(12A)	1.0077(7)	0.6180(6)	0.0687(5)
C(13A)	0.9926(8)	0.6481(6)	0.0015(5)
O(1B)	0.7428(5)	0.5514(3)	0.0028(3)
O(2B)	0.7729(5)	0.4485(4)	−0.1322(3)
O(3B)	0.8208(5)	0.5533(4)	−0.1011(3)
C(1B)	0.6972(7)	0.5437(5)	0.0575(5)
C(2B)	0.5979(7)	0.5639(5)	0.0520(4)
C(3B)	0.5552(7)	0.5547(5)	0.1075(5)
C(4B)	0.6054(7)	0.5240(5)	0.1650(5)
C(5B)	0.7052(8)	0.5069(6)	0.1682(5)
C(6B)	0.7553(8)	0.5174(5)	0.1159(5)
C(7B)	0.5385(7)	0.6007(5)	−0.0072(5)
C(8B)	0.5525(7)	0.5063(6)	0.2220(5)
C(9B)	0.4817(8)	0.5620(7)	0.2319(5)
C(10B)	0.4894(8)	0.4433(6)	0.2021(5)
C(11B)	0.6297(8)	0.4958(7)	0.2869(5)
C(12B)	0.7370(8)	0.4899(6)	−0.0324(5)
C(13B)	0.7777(7)	0.4957(5)	−0.0952(5)
C(14B)	0.8684(9)	0.5605(6)	−0.1603(5)
C(15B)	0.7907(8)	0.5749(7)	−0.2213(5)
O(1C)	0.6909(5)	0.7032(3)	−0.0004(3)
O(2C)	0.7598(5)	0.8047(4)	−0.0745(3)
O(3C)	0.7369(7)	0.7339(4)	−0.1611(4)
C(1C)	0.5986(7)	0.7187(5)	0.0162(4)
C(2C)	0.5910(7)	0.7815(5)	0.0428(4)
C(3C)	0.4985(8)	0.7986(5)	0.0592(4)
C(4C)	0.4171(8)	0.7538(5)	0.0504(4)
C(5C)	0.4312(7)	0.6922(5)	0.0258(4)
C(6C)	0.5247(7)	0.6726(5)	0.0092(4)
C(7C)	0.6789(8)	0.8276(5)	0.0613(5)
C(8C)	0.3167(7)	0.7750(6)	0.0678(5)
C(9C)	0.3387(8)	0.7990(6)	0.1400(5)
C(10C)	0.2399(8)	0.7196(6)	0.0604(6)
C(11C)	0.2728(9)	0.8340(7)	0.0239(5)
C(12C)	0.6909(8)	0.6938(6)	−0.0686(4)
C(13C)	0.7313(8)	0.7510(6)	−0.0996(4)
C(14C)	0.7671(10)	0.7962(9)	−0.2109(8)
C(15C)	0.8665(14)	0.7788(8)	−0.1859(6)
O(1D)	0.8925(5)	0.7851(3)	0.0827(3)
O(2D)	1.0772(5)	0.8487(4)	0.1364(4)
O(3D)	1.0187(5)	0.9405(4)	0.0803(3)
C(1D)	0.8431(7)	0.7897(5)	0.1359(4)
C(2D)	0.8977(7)	0.7631(5)	0.1968(4)
C(3D)	0.8485(8)	0.7648(5)	0.2491(5)
C(4D)	0.7530(8)	0.7886(5)	0.2456(5)
C(5D)	0.7022(7)	0.8113(5)	0.1833(4)
C(6D)	0.7446(7)	0.8092(5)	0.1285(4)
C(7D)	0.9991(8)	0.7298(5)	0.2053(5)
C(8D)	0.7021(8)	0.7857(6)	0.3052(5)
C(9D)	0.6899(10)	0.7151(6)	0.3222(5)
C(10D)	0.5998(9)	0.8202(6)	0.2910(5)
C(11D)	0.7723(9)	0.8210(7)	0.3653(5)
C(12D)	0.9136(8)	0.8478(6)	0.0587(5)
C(13D)	1.0135(9)	0.8766(5)	0.0972(5)
C(14D)	1.1111(8)	0.9755(6)	0.1110(5)
C(15D)	1.1009(11)	1.0443(7)	0.0887(6)

of a saturated hexane solution. We initially attempted to determine the structure of **5** with data collected at room temperature but as we could measure no 'observed' data with a $\theta > 15$ we were (not surprisingly) unable to determine the structure with these limited data. On cooling the data crystal to 123 K sufficient data in the θ-range 15–21 were obtained to allow us to determine the structure.

Crystal Data.—Compound **5** at 123 K, $C_{58}H_{76}O_{12}$, M = 965.2, monoclinic, a = 13.554(6), b = 20.095(9), c = 20.658(17) Å, β = 102.27(5)°, V = 5498(6) Å^3, Z = 4, D_x = 1.14 g cm^{-3}, $F(000)$ = 2080, λ(Mo-Kα) = 0.710 73 Å, μ(Mo-Kα) = 0.8 cm^{-1}, space group $P2_1/n$ uniquely from the systematic absences ($h0$ absent if $h + 2n + 1$; $0k0$ absent if $k = 2n + 1$).

A colourless crystal of **5** which measured 0.14 × 0.19 × 0.35 mm was used for the crystal structure analysis. The setting angles of 25 reflections with $10 < 2\theta < 27°$ were measured on a CAD4 diffractometer and used to determine cell constants and crystal orientation matrix. Intensities of reflections with indices h 0 to 13, k 0 to 20, l −26 to 26 with $2 < 2\theta < 42°$ were measured [ω–2θ scans; ω scan width (0.6 + 0.35 tan θ)°] with graphite monochromatised Mo-Kα radiation. Data collection was stopped at 2θ of 42° as no 'observed' reflections were being measured. Lorentz and polarisation corrections were applied to the data; the intensities of three standard reflections measured every 120 min remained constant and no decay correction was required. 6162 reflections were measured of which 5860 were unique (R_{int} 0.024), and the 2017 with $I > 1.5\sigma(I)$ were labelled observed and used in the structure analysis. The structure was solved by direct methods.[17] Initial refinement was by full-matrix least-squares calculations with isotropic thermal parameters. Difference maps had maxima in the expected locations for the H atoms and these were positioned geometrically (C–H 0.95 Å) and allowed for as riding atoms in subsequent refinement cycles. The carboxyl oxygen O3A was only 2.7 Å from proximal ether oxygen O1D and a difference map showed the carboxyl H atom clearly on the O3A ··· O1D line of centres; it was included in subsequent refinement cycles as a riding atom 0.95 Å from O3A on the O3A ··· O1D vector. For the final rounds of refinement, all non-H atoms were allowed anisotropic motion and block-diagonal least-squares methods were employed. Even at 123 K, it is clear that some of the ester and *tert*-butyl carbon atoms have large anisotropic motion or are slightly disordered; but there was no clear indication from difference maps of any distinct maxima which would have allowed us to refine a disordered model. At convergence, R = 0.063, R_w = 0.059, goodness-of-fit 1.39. The maximum shift/esd ratio in the final cycle was 0.02; the range of density in the final difference map was −0.27 to +0.33 e Å^{-3} (no chemically significant features). The weighting scheme used was of the form, $w = 1[(\sigma^2 F_o^2) + 0.0006(F_o)]$. All calculations were performed on a Silicon Graphics 4D-380 computer using the NRCVAX suite of programs.[17] Scattering factors and anomalous-dispersion corrections from International Tables for X-ray Crystallography.[18] A summary of the bond lengths is in Table 2 and atomic coordinates are in Table 3. Figs. 1 and 2 are views of molecule **5** prepared using ORTEPII[19] showing the crystallographic numbering scheme.

Additional material available from the Cambridge Crystallographic Data Centre (CCDC) comprises thermal parameters, calculated hydrogen coordinates and full details of molecular geometry.* Copies of the structure factor listing and the difference map section showing the hydrogen involved in the O–H ··· O hydrogen bond are available from either M. A. McK or G. F.

* For details of the CCDC deposition scheme, see 'Instructions for Authors', *J. Chem. Soc., Perkin Trans. 2*, 1992, Issue 1.

Acknowledgements

G. F. thanks NSERC for the award of an Operating Grant.

References

1 For comprehensive accounts of several aspects of the complexation chemistry of calixarenes, see (*a*) C. D. Gutsche, *Calixarenes*, vol. 1 in Monographs in Supramolecular Chemistry, ed. J. F. Stoddart, Royal Society of Chemistry, 1989; (*b*) V. Bohmer and J. Vicens, eds., *Topics in Inclusion Phenomena, Calixarenes, A Versatile Class of Macrocyclic Compounds*, Kluwer Academic Publishers, 1990.

2 M. A. McKervey and M. J. Schwing-Weill, ref. 1(*b*), pp. 149–172; R. Ungaro and A. Pochini, ref. 1(*b*), pp. 127–147.

3 M. A. McKervey, E. M. Seward, G. Ferguson, B. L. Ruhl and S. J. Harris, *J. Chem. Soc., Chem. Commun.*, 1985, 388; S. K. Chang and I. Cho, *Chem. Lett.*, 1984, 477; S. K. Chang and I. Cho, *J. Chem. Soc., Perkin Trans. 1*, 1986, 211; A. Arduini, A. Pochini, S. Reverberi, R. Ungaro, C. D. Andretti and F. Ugozzoli, *Tetrahedron*, 1986, **42**, 2098; F. Arnaud-Neu, E. M. Collins, M. Deasy, G. Ferguson, S. J. Harris, B. Kaitner, A. J. Lough, M. A. McKervey, E. Marques, B. L. Ruhl, M. J. Schwing-Weill and E. M. Seward, *J. Am. Chem. Soc.*, 1989, **111**, 8681.

4 G. Ferguson, B. Kaitner, M. A. McKervey and E. M. Seward, *J. Chem. Soc., Chem. Commun.*, 1987, 584.

5 R. Ungaro, A. Pochini and G. D. Andreetti, *J. Incl. Phenom.*, 1984, **2**, 199.

6 S. K. Chang, S. K. Kwon and I. Cho, *Chem. Lett.*, 1987, 947; A. Arduini, E. Ghidini, A. Pochini, R. Ungaro, D. G. Andreetti, G. Calestani and F. Ugozzoli, *J. Incl. Phenom.*, 1988, **6**, 119; F. Arnaud-Neu, M. J. Schwing-Weill, K. Ziat, S. Cremin, S. J. Harris and M. A. McKervey, *New J. Chem.*, 1991, **15**, 33.

7 For a preliminary account of this work, see V. Bohmer, W. Vogt, S. J. Harris, R. G. Leonard, E. M. Collins, M. Deasy, M. A. McKervey and M. Owens, *J. Chem. Soc., Perkin Trans. 1*, 1990, 431.

8 F. Arnaud-Neu, M. J. Schwing-Weill and P. Schwinte, unpublished results.

9 See examples in ref. 3 and C. D. Andreetti and F. Ugozzoli in ref. 1(*b*), pp. 87–123.

10 A. Wolff, V. Bohmer, W. Vogt, F. Ugozzoli and G. D. Andreetti, *J. Org. Chem.*, 1990, **55**, 5665.

11 V. Bohmer, W. Vogt, H. Goldmann, M. A. McKervey, M. Owens, S. Cremin and E. M. Collins, *J. Org. Chem.*, 1990, **55**, 2569.

12 F. Arnaud-Neu, V. Bohmer, L. Guerra, M. A. McKervey, E. F. Paulus, A. Rodriguez, M. J. Schwing-Weill, M. Tabatabai and W. Vogt, *J. Phys. Org. Chem.*, in press.

13 E. M. Collins, M. A. McKervey, E. Madigan, M. B. Moran, M. Owens, G. Ferguson and S. J. Harris, *J. Chem. Soc., Perkin Trans. 1*, 1991, 3137.

14 M. A. McKervey, M. Owens, H.-R. Schulten, W. Vogt and V. Bohmer, *Angew. Chem. Int., Ed. Engl.*, 1990, **29**, 280.

15 G. Barrett, S. J. Harris and M. A. McKervey, *J. Chem. Soc., Chem. Commun.*, 1991, 1224.

16 D. Diamond, S. J. Harris, M. McCarrick, Bei Wu, G. Barrett and M. A. McKervey, unpublished results.

17 E. J. Gabe, Y. Le Page, J.-P. Charland, F. L. Lee and P. S. White, *J. Appl. Crystallogr.*, 1989, **22**, 384.

18 International Tables for X-ray Crystallography, 1974, vol. IV, Kynoch Press, Birmingham, UK. (Present distributor Kluwer Academic Publishers, Dordrecht, The Netherlands.)

19 C. K. Johnson, ORTEPII, Report ORNL-5138, Oak Ridge National Laboratory, Tennessee, USA, 1976.

Paper 2/01725C
Received 1*st April* 1992
Accepted 15*th May* 1992